doi:10.1093/brain/awaa206 BRAIN 2020: 143; 2406–2420 | 2406

BRAIN
A JOURNAL OF NEUROLOGY

Loss of supervillin causes myopathy with myofibrillar disorganization and autophagic vacuoles

Carola Hedberg-Oldfors,[1,*] Robert Meyer,[2,*] Kay Nolte,[3,*] Yassir Abdul Rahim,[1] Christopher Lindberg,[4] Kristjan Karason,[5] Inger Johanne Thuestad,[6] Kittichate Visuttijai,[1] Mats Geijer,[7,8] Matthias Begemann,[2] Florian Kraft,[2] Eva Lausberg,[2] Lea Hitpass,[9] Rebekka Götzl,[10] Elizabeth J. Luna,[11] Hanns Lochmüller,[12,13] Steffen Koschmieder,[14] Michael Gramlich,[15] Burkhard Gess,[16] Miriam Elbracht,[2] Joachim Weis,[3] Ingo Kurth,[2] Anders Oldfors[1] and Cordula Knopp[2]

*These authors contributed equally to this work.

The muscle specific isoform of the supervillin protein (SV2), encoded by the *SVIL* gene, is a large sarcolemmal myosin II- and F-actin-binding protein. Supervillin (SV2) binds and co-localizes with costameric dystrophin and binds nebulin, potentially attaching the sarcolemma to myofibrillar Z-lines. Despite its important role in muscle cell physiology suggested by various *in vitro* studies, there are so far no reports of any human disease caused by *SVIL* mutations. We here report four patients from two unrelated, consanguineous families with a childhood/adolescence onset of a myopathy associated with homozygous loss-of-function mutations in *SVIL*. Wide neck, anteverted shoulders and prominent trapezius muscles together with variable contractures were characteristic features. All patients showed increased levels of serum creatine kinase but no or minor muscle weakness. Mild cardiac manifestations were observed. Muscle biopsies showed complete loss of large supervillin isoforms in muscle fibres by western blot and immunohistochemical analyses. Light and electron microscopic investigations revealed a structural myopathy with numerous lobulated muscle fibres and considerable myofibrillar alterations with a coarse and irregular intermyofibrillar network. Autophagic vacuoles, as well as frequent and extensive deposits of lipoproteins, including immature lipofuscin, were observed. Several sarcolemma-associated proteins, including dystrophin and sarcoglycans, were partially mis-localized. The results demonstrate the importance of the supervillin (SV2) protein for the structural integrity of muscle fibres in humans and show that recessive loss-of-function mutations in *SVIL* cause a distinctive and novel myopathy.

1 Department of Pathology and Genetics, Sahlgrenska Academy, University of Gothenburg, Gothenburg, Sweden
2 Institute of Human Genetics, Medical Faculty, RWTH Aachen University, Aachen, Germany
3 Institute of Neuropathology, Medical Faculty, RWTH Aachen University, Aachen, Germany
4 Department of Neurology, Neuromuscular Centre, Sahlgrenska University Hospital, Gothenburg, Sweden
5 Department of Cardiology and Transplant Institute, Sahlgrenska University Hospital, Gothenburg, Sweden
6 Department of Pediatrics, Skane University Hospital, Malmo, Sweden
7 Department of Radiology, Sahlgrenska Academy, University of Gothenburg, Gothenburg, Sweden
8 Department of Clinical Sciences, Lund University, Lund, Sweden
9 Department of Diagnostic and Interventional Radiology, Medical Faculty, RWTH Aachen University, Aachen, Germany
10 Department of Plastic Surgery, Hand and Burn Surgery, Medical Faculty, RWTH Aachen University, Aachen, Germany
11 Division of Cell Biology and Imaging, Department of Radiology, University of Massachusetts Medical School, Worcester, USA
12 Children's Hospital of Eastern Ontario Research Institute, Division of Neurology, Department of Medicine, The Ottawa Hospital, Ottawa, Canada

Received January 25, 2020. Revised April 16, 2020. Accepted May 7, 2020

13 Brain and Mind Research Institute, University of Ottawa, Ottawa, Canada
14 Department of Hematology, Oncology, Hemostaseology and Stem Cell Transplantation, Medical Faculty, RWTH Aachen University, Aachen, Germany
15 Department of Invasive Electrophysiology, Medical Faculty, RWTH Aachen University, Aachen, Germany
16 Department of Neurology, Medical Faculty, RWTH Aachen University, Aachen, Germany

Correspondence to: Anders Oldfors
Department of Pathology and Genetics, Sahlgrenska Academy, University of Gothenburg
Gothenburg, Sweden
E-mail: anders.oldfors@gu.se

Correspondence may also be addressed to: Cordula Knopp
Institute of Human Genetics, Medical Faculty, RWTH Aachen University, Aachen, Germany
E-mail: cknopp@ukaachen.de

Keywords: *SVIL*; supervillin; myopathy; costameric protein; cardiac disease

Abbreviations: ERK = extracellular-signal-regulated kinase; LC3 = microtubule-associated protein 1A/1B-light chain 3; SV2 = supervillin isoform 2, muscle specific

Introduction

Supervillin, encoded by the *SVIL* gene, is a large eukaryotic protein from the villin/gelsolin superfamily of actin-binding proteins (Pestonjamasp *et al.*, 1997) that is involved in many cellular processes. Among others, supervillin regulates cytokinesis (Smith *et al.*, 2010, 2013), cell adhesion (Takizawa *et al.*, 2006) and cell motility (Fang *et al.*, 2010) and promotes cell survival through control of p53 levels (Fang and Luna, 2013). Supervillin mRNAs are expressed in most human tissues, but are most abundant in skeletal muscle, followed by the heart and organs containing secretory or smooth muscle cells (Pope *et al.*, 1998). In cardiac and skeletal muscle, the 250-kDa muscle-specific isoform of supervillin (SV2), also called archvillin, is predominantly expressed (Pope *et al.*, 1998; Oh *et al.*, 2003; Fang and Luna, 2013). Supervillin (SV2) is localized at the ends of differentiating myotubes (Oh *et al.*, 2003) and plays a role in myofibrillar assembly (Lee *et al.*, 2007). There is evidence for co-localization and interaction of supervillin (SV2) with structural proteins in costameres and sarcomeres, which are important components of cardiac and skeletal muscle cells (Oh *et al.*, 2003; Lee *et al.*, 2007, 2008; Spinazzola *et al.*, 2015). Among others, there are interactions with nebulin, dystrophin and γ-sarcoglycan, for which distinct and often severe human muscular disorders are well known. For example, mutations in nebulin account for about 50% of patients with congenital nemaline myopathy (Romero and Clarke, 2013). Genetic variants in costameric proteins, such as dystrophin, cause cardiac and skeletal muscle disorders (Nigro and Piluso, 2015). Mutations in components of the sarcoglycan complex likewise cause limb-girdle muscular dystrophies, which are variably associated with cardiomyopathy (Jaka *et al.*, 2015).

Despite the interaction of supervillin (SV2) with costameric and sarcomeric proteins, no muscular disease associated with *SVIL* mutations has so far been described. Here, we report four patients from two unrelated families with homozygous loss-of-function mutations in *SVIL*. The patients presented with myopathy and mild cardiac involvement and share a characteristic muscle pathology with lobulated fibres and other structural abnormalities.

Material and methods

Patients and clinical evaluation

Two families with two affected siblings with myopathy, respectively, were investigated clinically, morphologically and genetically. Family 1 originates from Lebanon and Family 2 from Turkey. The study complied with the Declaration of Helsinki, and informed consent was obtained from all individuals included in this study. Medical history taking and physical examination were focused on neuromuscular and cardiac symptoms and signs. A summarized overview of the clinical phenotypes of all four patients is provided in Table 1.

Muscle MRI

Magnetic resonance examinations were performed in all four patients according to protocols described in the Supplementary material.

Morphological analysis

Skeletal muscle biopsy was performed in all four patients. Specimens were snap-frozen in liquid propane chilled with liquid nitrogen for cryostat sectioning and histochemistry, and fixed in buffered glutaraldehyde for electron microscopy. Standard techniques were used for enzyme histochemistry, immunohistochemistry and electron microscopy (Dubowitz *et al.*, 2013). For immunohistochemistry investigations, fresh frozen sections were incubated with primary

Table 1 Clinical phenotypes and results from laboratory investigations in the patients

	Family 1 Country of origin: Lebanon		Family 2 Country of origin: Turkey	
	Patient III:1	**Patient III:5**	**Patient III:2**	**Patient III:3**
Gender	Male	Male	Female	Male
Age at onset/last examination	Childhood/27 years	Adolescence/17 years	At birth/41 years	Infancy/34 years
Initial symptoms	Thin muscles particularly lower legs since childhood	Increased fatigue at exercise	Congenital contractures of hips and elbows	Tiptoe walking in infancy
Clinical complaints	Between 20 to 24 years of age episodic weakness, muscle pain and muscle fatigue at exercise; since then asymptomatic	Increased fatigue at exercise	Muscle pain (neck and shoulders), muscular cramps (lower legs, feet), painful cramping when remaining in the same position for long	Muscular cramps (lower legs, feet), painful cramping when remaining in the same position for long, mild weakness when working above head height
Clinical examination				
Physical signs	Wide neck, anteverted shoulders, prominent trapezius and latissimus dorsi muscles, thin lower legs, slight syndactyly between fingers, sandal gap	Wide neck, muscles of extremities hypertrophic proximal compared to distal, hypertrophic lumbar back muscles, mild syndactyly between fingers, sandal gap	Wide neck and malposition of shoulder girdle (hypertrophic and rigid trapezius muscle, anteverted shoulders, hyperkyphosis), mandibular protrusion	Wide neck and malposition of shoulder girdle (hypertrophic and rigid. trapezius muscle, anteverted shoulders, hyperkyphosis), mandibular protrusion
Contractures	Long finger flexors, slight shortening of Achilles tendons	None	Knee, ankles, elbow, fingers	Knee, ankles, elbow, fingers
Percussion myotonia	NA	NA	Deltoid and biceps bracchii muscle	Deltoid and biceps bracchii muscle
Muscle strength	Normal	Normal	Normal	Normal
Further examination				
NCV	Normal	Normal	Normal	Normal
EMG	Myopathic in quadriceps muscle, normal in deltoid and interosseous dorsi muscles	Myopathic	Normal in deltoid muscle	Normal in deltoid muscle
Whole-body MRI	Normal muscular structure	Normal muscular structure	Normal muscular structure	Normal muscular structure
ECG	Q waves in aVL, I and –aVR, T-inversions in aVF and 3, increased QRS amplitudes	Tendency towards left ventricular hypertrophy	Prolonged QTc-time (501 ms)	T-inversions in aVF and 3
Holter-ECG	Normal	NA	Normal	NA
Echocardiography	Normal	Slightly hypertrophic left ventricular wall	Normal (slight tricuspid regurgitation)	Slightly hypertrophic left ventricular wall, slight tricuspid regurgitation
Cardio-MRI	Increased basal wall thickness	Normal	Normal	Normal
Creatine kinase	3 × UNR	2-4 × UNR	2–3 × UNR	2 × UNR
Troponin T (ref. val. < 14 ng/l)	20–30 ng/l	13–158 ng/l	15 ng/l	8 ng/l
Haemostasis and coagulation investigation	NA	NA	Normal	Normal
Muscle biopsy	Structural myopathy with prominent lobulated type 1 fibres, myofibrillar disintegration and signs of altered proteostasis/impaired autophagy			
DNA analysis	c.4812C>A (hom)	c.4812C>A (hom)	c.3578_3579del (hom)	c.3578_3579del (hom)
Protein change	p.Tyr1604*	p.Tyr1604*	p.Val1193Glufs*46	p.Val1193Glufs*46

hom = homozygous; NA = not assessed; UNR = upper normal range.

antibodies according to Supplementary Table 1A. Controls used in this study included muscle biopsies from age-matched individuals, investigated for muscle complaints but in whom the investigations excluded a muscle disease.

Molecular genetic analysis

For Family 1, exome sequencing target enrichment was performed on genomic DNA from Patients III:1 and III:5 using the Sure SelectXT Human All Exon kit version 6 (Agilent Technologies), with sequencing on the HiSeq4000 platform (Illumina). The paired-end reads were aligned to the reference genome (hg19). Based on the assumption of a recessive inherited disease a search for potential compound heterozygous or homozygous variants in genes possible to be associated with myopathy was performed. Population frequencies were estimated using the genome aggregation database (gnomAD), last accessed in June 2019. The Combined Annotation-Dependent Depletion (CADD) tool (version v1.4) was used as an *in silico* prediction algorithm to predict the pathogenicity of the variants identified. Variants with CADD scores >20 with allele frequencies <1% were evaluated further. Candidate variants were confirmed by Sanger sequencing and segregation studies were performed with available DNA samples.

For RNA studies, total RNA was isolated from frozen skeletal muscle from Patients III : 1 and III : 5 using the RNeasy® Fibrous Tissue Mini Kit (Qiagen). RNA was reverse transcribed with the QuantiTect reverse transcription kit (Qiagen), and cDNA was analysed by PCR and Sanger sequencing. The forward and reverse primers were designed to hybridize to different exons that were separated by large

introns to generate a specific PCR-product on cDNA (Supplementary Fig. 1B and C). Primer sequences and PCR conditions are described in the Supplementary material.

For Family 2, exome sequencing was performed with the DNA from peripheral blood of Patients III:2 and III:3. Enrichment was done with an Illumina Enrichment Kit (Nextera Rapid Capture Exome v1.2). The exome library was sequenced on a NextSeq500 Sequencer with 2 × 75 cycles. FastQ files were generated with bcl2fastq2 (Illumina, San Diego, CA, USA). Primary alignment, indel realignment and variant calling were performed by using an in-house pipeline based on SeqMule (Guo *et al.*, 2015). Variant calling was done by three different variant callers (GATKLite, SAMtools, FreeBayes). Genome version hg19 was used for the alignment. Only variants called by at least two variant callers were included in the final variant file. Average coverage in the target region was 80× (Patient III:2)/89× (Patient III:3), with 89% (Patient III : 2)/91% (Patient III:3) above 20× coverage. For variant annotation and prioritization of variants KGGSeq was used (Li *et al.*, 2012). Synonymous variants and variants with a minor allele frequency (MAF) higher than 0.75% in public databases (i.e. gnomAD, ExAC, 1000 Genomes Project, ESP) were excluded from further analysis.

Based on known consanguinity of the parents, homozygous variants were prioritized for investigation of the exome sequencing data. The remaining 17 homozygous variants shared by both siblings were filtered for potential loss-of-function, putative splicing variants and missense variants that were predicted to be probably pathogenic using different tools (CADD, PolyPhen, MutationTaster). Only putative loss of function variants and variants with a CADD score higher than 20 were kept. Variants were confirmed by Sanger sequencing on a 3500 Genetic Analyzer platform (Applied Biosystems). Segregation analysis was performed in the mother, whereas DNA of the father was not available for further testing.

Western blot

For Family 1, western blot was performed on protein extracted from cryostat sections of muscle biopsy specimens from both patients (Patients III:1 and III:5). The supernatants (including protein) were loaded and separated on a 3 to 8% Tris-Acetate gel (Novex; Life Technologies), followed by electroblotting. The membranes were incubated with two different antibodies against human supervillin (anti-SVIL; Atlas antibodies; HPA020138, 1:500, epitope in the middle part of the protein aa 847-984; CPTC-SVIL-3, 1:10, epitope in the N-terminus of the protein amino acids 1–220) as primary antibodies. The epitopes of these antibodies are located N-terminal to the location of the identified mutation. The SuperSignal™ West Femto Maximum Sensitivity Substrate (Life Technologies) was used for antibody detection.

For Family 2, western blot was performed on protein extracted from a fresh frozen piece of the deltoid muscle from both patients (Patients III:2 and III:3) using T-PER buffer (Pierce). The lysates were subjected to SDS-polyacrylamide gel electrophoresis (PAGE) under reducing conditions and transferred to polyvinylidene difluoride-membranes (Millipore). The blots were incubated with the appropriate antibody in TBS-T containing 3% BSA overnight at 4°C, respectively. Primary antibodies and dilutions are listed in Supplementary Table 1B. Controls used in this study included muscle biopsies from age-matched individuals, investigated for muscle complaints but in whom the investigations excluded a muscle disease. An extended protocol can be found in the Supplementary material.

Data availability

Data are available upon request.

Results

Clinical reports

Family 1

Patient III:1 in Family 1 was a 27-year-old male and first child of consanguineous healthy parents (first degree cousins) of Lebanese ancestry. Since childhood, he has had thin muscles especially affecting the lower legs without apparent weakness. Between 20 and 24 years of age, he had experienced episodic muscle pain, weakness and fatigue. These episodes were most evident in his arms and legs in the beginning of the day, lasting from one month to several months and without any apparent triggering or associated factors. Neurological examination at age 27 revealed no muscle weakness, but the lower legs were thin, the medial parts of the gastrocnemius muscles were atrophic (Fig. 1). He had a wide neck, anteverted shoulders, prominent trapezius and latissimus dorsi muscles and a tendency to thoracic kyphosis. He had slight shortening of the Achilles tendons, and slight contractures of his long finger flexors. Slight syndactyly was observed between fingers and a tendency to sandal gap widening between the first and second toe. EMG of the vastus lateralis was borderline myopathic as found on the turns amplitude analysis of the interference pattern. EMG was normal in the deltoid muscle and the interosseus dorsi muscles of the hands. At age 20 years, he was examined because of recurrent sharp chest pains. His ECG showed Q waves in aVL, I and aVR, T-inversions in aVF and III and increased QRS amplitudes in the chest leads, suggesting left ventricular hypertrophy. A cardiopulmonary exercise test (CPET) was prematurely terminated due to leg fatigue and showed reduced exercise capacity, 192 W, 70% of the reference value. Twenty-four-hour Holter monitoring and echocardiography were normal. A cardiac MRI (CMR) at age 27 showed increased basal wall thickness (30 mm) consistent with hypertrophy and a small ventricular diverticulum, but otherwise adequate systolic ventricular performance and normal valvular function. There were no signs of atrial abnormalities.

Figure 1 Clinical picture of Family 1. (**A–D**) Patient III:5. (**E–H**) Patient III:1. (**A** and **B**) Hypertrophic trapezius muscles and wide neck. Limb muscles are hypertrophic proximally as compared to distally in both arms and legs and the lumbar back muscles are prominent. (**C** and **D**) Syndactyly is present between all fingers and the feet show sandal gap sign. (**E**) Wide neck, anteverted shoulders, prominent trapezius and latissimus dorsi muscles and a tendency to thoracic kyphosis. (**F**) The lower legs are thin with reduced size of the medial parts of the gastrocnemius muscles and a tendency to sandal gap widening between the first and second toe. (**G** and **H**) Slight syndactyly is present between fingers and slight contractures of the long finger flexors.

Laboratory tests revealed a persistent increase in high-sensitive cardiac troponin T 20–30 ng/l (reference value <14 ng/l), serum creatine kinase (CK) 18–22 μkat/l (reference interval 0.80–6.7 μkat/l), CK-MB 32–36 μg/l (reference value <5 μg/l) and myoglobulin 178 μg/l (reference value <90 μg/l). N-terminal prohormone of brain natriuretic peptide (NT-proBNP) was normal 130–250 ng/l (reference value <300 ng/l).

MRI showed a symmetrical representation of all muscles. In the right semimembranosus muscle, there was a marked high signal on the fat-suppressed T_2-weighted sequence representing oedema, with a slight fatty infiltration in the medial half of the muscle. On the left, there was a superficial marginal oedema in the same muscle without fatty infiltration. Otherwise, no evidence of intramuscular oedema or fatty degeneration could be found. The distribution of the muscle bulk corresponded with the clinical assessment, and there were no signs of fatty replacement of the relatively thin muscles of the lower legs and distal arms.

Patient III:5 was a 17-year-old male and the younger brother of Patient III:1. Since age 12 years he had experienced increased fatigue and shortness of breath at exercise. At age 13 years he experienced an episode of syncope during physical activity. He complained of chest pains, and ECG showed a tendency towards left ventricular hypertrophy, which was confirmed by echocardiography, showing a slightly hypertrophic left ventricular wall. A subsequent cardiac MRI showed a normal size of the heart chambers and normal function. No cardiac fibrosis was seen. Later, ergometry and spirometry showed normal results. Blood tests showed elevated levels of troponin T; 134, 158, 72, 50 ng/l (reference value <15 ng/l) measured over the course of 3 days, and later at follow-up 13 and 31 ng/l. NT-proBNP at corresponding dates measured 142, 183, 285 and 80 ng/l (reference value <100 ng/l) and later at follow-up 65 and 90 ng/l. The serum creatine kinase level was continuously slightly elevated, 15-30 μkat/l (reference interval 0.80–6.7 μkat/l).

Neurological examination showed no joint contractures. His neck was wide and the proximal limb muscles were found to be hypertrophic as compared to the distal ones in both arms and legs (Fig. 1). The lumbar back muscles were also hypertrophic. Mild syndactyly was found between all fingers and his feet showed sandal gap sign. Muscle strength was normal in all muscle groups, though he was somewhat slower than expected for his age in the 6-min walk test. The deep tendon reflexes were absent in the arms, whereas they were normal in the legs, without any apparent explanation for the discrepancy. The facial muscles were unaffected. EMG indicated myopathy, and nerve conduction studies were normal.

MRI of the muscles in the limbs, thorax, abdomen, and pelvis showed normal muscle structure. MRI showed a symmetrical representation of all muscles without circumscribed atrophies. No evidence of intramuscular oedema or fatty degeneration could be found. The thigh muscles were better developed than the muscles in the lower legs corresponding with the clinical picture. The dorsal shoulder musculature was hypertrophic, also corresponding with the clinical assessment.

Family 2

The index patient (Patient III:2), a 41-year-old female, showed dysmorphism of the neck and shoulders in combination with muscular rigidity and myalgia (Fig. 2). She was the first child of consanguineous healthy parents (first-degree cousins) of Turkish origin. Her younger 34-year-old brother (and only sibling) (Patient III:3) (Fig. 2) was similarly affected while her 11-year-old daughter was healthy. Further family history was unremarkable; there were no further family members affected by neuromuscular disorders.

Both patients presented with a history of a neuromuscular disorder. The female patient reported congenital contractures of the hips and elbows while her brother reported tiptoe walking in infancy as the initial symptom. No significant delay in achieving motor milestones was reported and cognitive function was normal. Both patients had received physiotherapy since infancy. At the time of first presentation at our clinic at the age of 41 (Patient III:2) and 34 (Patient III:3) years, respectively, they complained about muscle pain especially of the neck and shoulders, muscle cramps predominantly affecting the lower legs and feet as well as painful cramping when remaining in the same position for long. Both patients described slowly progressive muscular rigidity and contractures leading to pain and limited mobility.

Figure 2 Clinical picture of Family 2. (**A**, **B** and **F**) Patient III:2. (**C**–**E** and **G**) Patient III:3. Wide neck due to hypertrophic M. trapezius, malposition of shoulder girdle with anteverted shoulders, hyperkyphosis (**A**–**D**), limited range of motion and contractures of elbows (**E**), contractures of long finger flexors (**F**) and contractures of knees and Achilles tendons (**G**).

However, motor strength has remained stable in both patients until today. In early adulthood, both patients underwent mandibular osteotomy of jawbone because of mandibular protrusion.

On physical examination both patients showed a broad neck and malposition of shoulder girdle including a hypertrophic and rigid trapezius muscle, anteverted shoulders and a hyperkyphosis of the thoracic spine accompanied by a limited range of motion (Fig. 2). Furthermore, there were bilateral contractures of the elbows, the long finger flexors (female > male), the knees and the Achilles tendons. Clinical examination did not reveal any obvious reduction of muscle strength. There was no facial weakness, ptosis or ophthalmoplegia. Bilateral percussion myotonia in the area of the deltoid and biceps brachii muscles was present in both patients (male > female). No rippling was observed. There were no myotonic reactions noticeable in further body regions. The deep tendon reflexes were normal.

Laboratory examination showed mildly elevated CK levels in both patients (Patient III:2: 4.8–5.8 μkat/l, Patient III:3: 5.3–5.5 μkat/l, reference value <2.8 μkat/l). Nerve conduction studies and electromyography revealed no irregularities in the patients. X-ray of the cervical and thoracic spine revealed a diminished lordosis of the cervical spine and an enhanced kyphosis and scoliosis of the thoracic spine in the female patient. Whole-body MRI focusing on the muscular anatomy showed a low and unspecific signal increase in the medial gastrocnemius head as well as in the left distal soleus muscle in Patient III:2. These MRI signal alterations were judged as unspecific, as they appear relatively commonly in these muscles without clinical significance and Patient III:2 had no clinical symptoms in leg function and force. Otherwise, MRI examinations of both siblings showed a symmetrical representation of all muscles without circumscribed atrophies. No evidence of intramuscular oedema or fatty degeneration could be found.

In the male patient, echocardiography showed a slightly hypertrophic left ventricular wall, but cardiac MRI did not show any structural cardiac involvement in either of the patients. However, in the female patient, ECG and Holter-ECG revealed a prolonged QT interval (QTc 501 ms); the patient did not take any medication. High-sensitive cardiac troponin T was normal in the male patient (8 ng/l) and slightly above the reference value in the female patient (15 ng/l, reference value < 14 ng/l). NT-proBNP was elevated in both patients (female patient 935 pg/ml, reference value <130 pg/ml; male patient 312 pg/ml, reference value <86 pg/ml). A comprehensive investigation of haemostasis and coagulation was normal in both patients.

Muscle histopathology

Family 1

Muscle biopsy showed structurally altered muscle fibres in both siblings, with coarse and irregular intermyofibrillar network and some ring fibres. In multiple regions groups of muscle fibres showed small vacuoles and internal nuclei. Occasional rimmed vacuoles were observed and also groups of fibres with protein aggregates in Patient III:1 (Fig. 3A and B). Many fibres were lobulated, which was the most apparent change (Fig. 3C). By electron microscopy, the vacuoles, some of which appeared as invaginations, were partly delimited by a sarcolemma-like membrane, but most appeared as autophagic vacuoles with cellular debris (Fig. 3D). Groups of fibres demonstrated Z-disc alterations with flag-like extensions and more widespread protein aggregates (Fig. 3E and F). By immunohistochemistry, vacuoles contained sarcolemma-associated proteins, such as α-sarcoglycan (Fig. 4A). Caveolin-3 marked some of the vacuoles and also showed a diffuse cytoplasmic immunoreactivity in occasional fibres, although the overall immunohistochemical staining was variably reduced, especially in the elder brother (Fig. 4B). Dystrophin was partly internalized (Fig. 4C) and desmin appeared to be partly accumulated, especially in the subsarcolemmal regions (Fig. 4D). Markers of autophagocytosis, lysosomal associated membrane protein 2 (LAMP2) and microtubule-associated protein 1A/1B-light chain 3 (LC3), were upregulated in some fibres (Fig. 4E and F). Staining for supervillin using the CPTC-SVIL-3 antibody from the Developmental Studies Hybridoma Bank (DSHB) showed a weak positive staining localized mainly to the sarcolemmal region in controls but was completely absent in both brothers (Fig. 4G).

Family 2

In both siblings, the muscle biopsy showed a moderately broadened muscle fibre calibre spectrum with numerous partially atrophic muscle fibres with diameters between 20 and 35 μm, but rarely less than 10 μm. There were no clearly hypertrophic muscle fibres (Fig. 5A). The partially atrophic muscle fibres had septa-like constrictions originating from the sarcolemma, which gave these fibres a lobulated profile, and there was prominent oxidative enzyme activity in these fibres (Fig. 5B). In addition, some muscle fibres had cushion-shaped, partially cap-like subsarcolemmal basophilic zones with granular content. ATPase reaction revealed that the partially atrophic, lobulated muscle fibres were almost exclusively of fibre type 1 (Fig. 5C). There was no evidence of necrotic muscle fibres. By electron microscopy, myofibrillary alterations of varying degree could be seen in several muscle fibres. Sarcoplasmic masses were frequently observed, including non-membrane-bound glycogen, mitochondria, and autophagic material (Fig. 5D). Several muscle fibres showed a subsarcolemmal accumulation of non-enlarged mitochondria. Accumulations of circumscribed granular or globoid deposits were frequent, probably consisting of immature lipofuscin and other lipoprotein deposits (Fig. 5E). Rarely, mature nemalin rods were observed (Fig. 5F and G). By immunohistochemistry, α-sarcoglycan appeared focally accumulated in the subsarcolemmal region and also internally in several fibres (Fig. 6A). Reduced caveolin-3 staining was observed in many fibres, especially small ones (Fig. 6B). Dysferlin was atypically present in non-sarcolemmal structures in some fibres (Fig. 6C), and desmin was focally

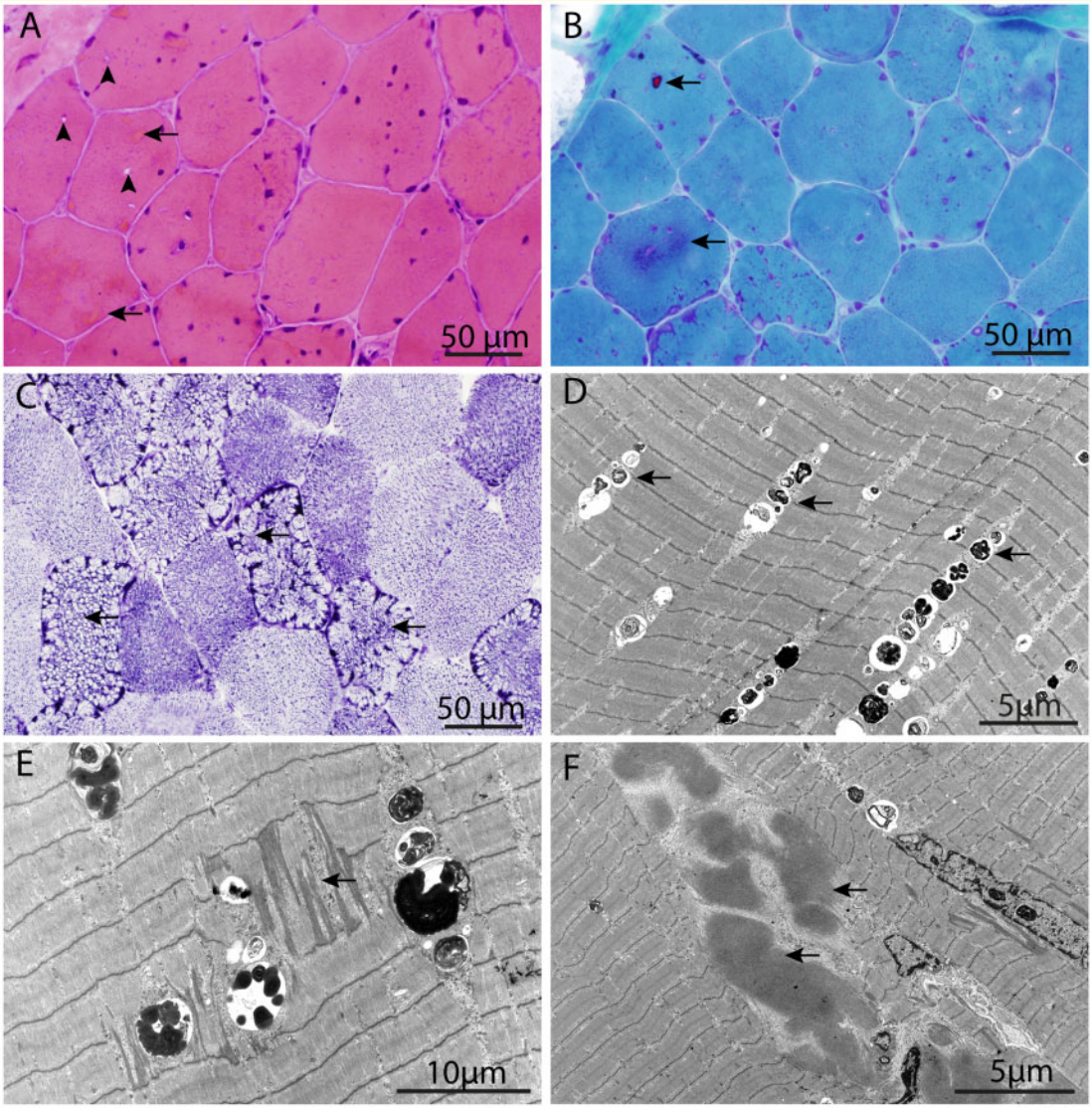

Figure 3 Biopsy from the vastus lateralis muscle of Patient III:1 in Family 1, as visualized by light (A–C) and electron microscopy (D–F). (**A**) Marked structural changes in groups of muscle fibres with internalized nuclei, eosinophilic protein aggregates (arrows) and multiple small vacuoles (arrowheads) (haematoxylin and eosin). (**B**) Some protein aggregates are purple in Gomori trichrome staining and others are dark green (arrows). (**C**) The intermyofibrillar network is deranged and partly unusually coarse (arrows). Many fibres appear lobulated which was the overall major alteration in the muscle biopsy (nicotinamide adenine dinucleotide tetrazolium reductase, NADH-TR). (**D**) In groups of muscle fibres, there are numerous autophagic vacuoles with membranous degradation products (arrows). (**E**) Focal disruption of the normal sarcomere structures (arrow) and autophagic vacuoles appearing together. (**F**) Large amorphous and partly fibrillar protein aggregates (arrows).

accumulated (Fig. 6D). There was subsarcolemmal accumulation of LC3 immunoreactivity and internal LC3-positive granular and vacuolar structures were also present in different muscle fibres (Fig. 6E and F). Sequestosome 1 (p62) was present under the sarcolemma in lobulated fibres and in autophagic vacuoles (Fig. 6G).

Molecular genetic analysis and western blotting

All affected patients from both families shared rare homozygous mutations in the supervillin gene (*SVIL;* OMIM: *604126, transcript NM_021738.2). Family 1 harboured a nonsense mutation in exon 26, c.4812C>A; p.Tyr1604*, which was not reported in genome databases (i.e. ExAC, gnomAD, 1000 Genomes Project, dbSNP151, ESP) (Fig. 7A, C and Supplementary Fig. 1A). Expression analysis of *SVIL* cDNA from skeletal muscle of Patients III:1 and III:5 from Family 1 showed lower *SVIL* transcript levels in the patient samples relative to control samples (Supplementary Fig. 1B and C). This result suggests that the transcripts were to a large extent degraded by nonsense-mediated mRNA decay, as expected by the introduction of a premature stop codon.

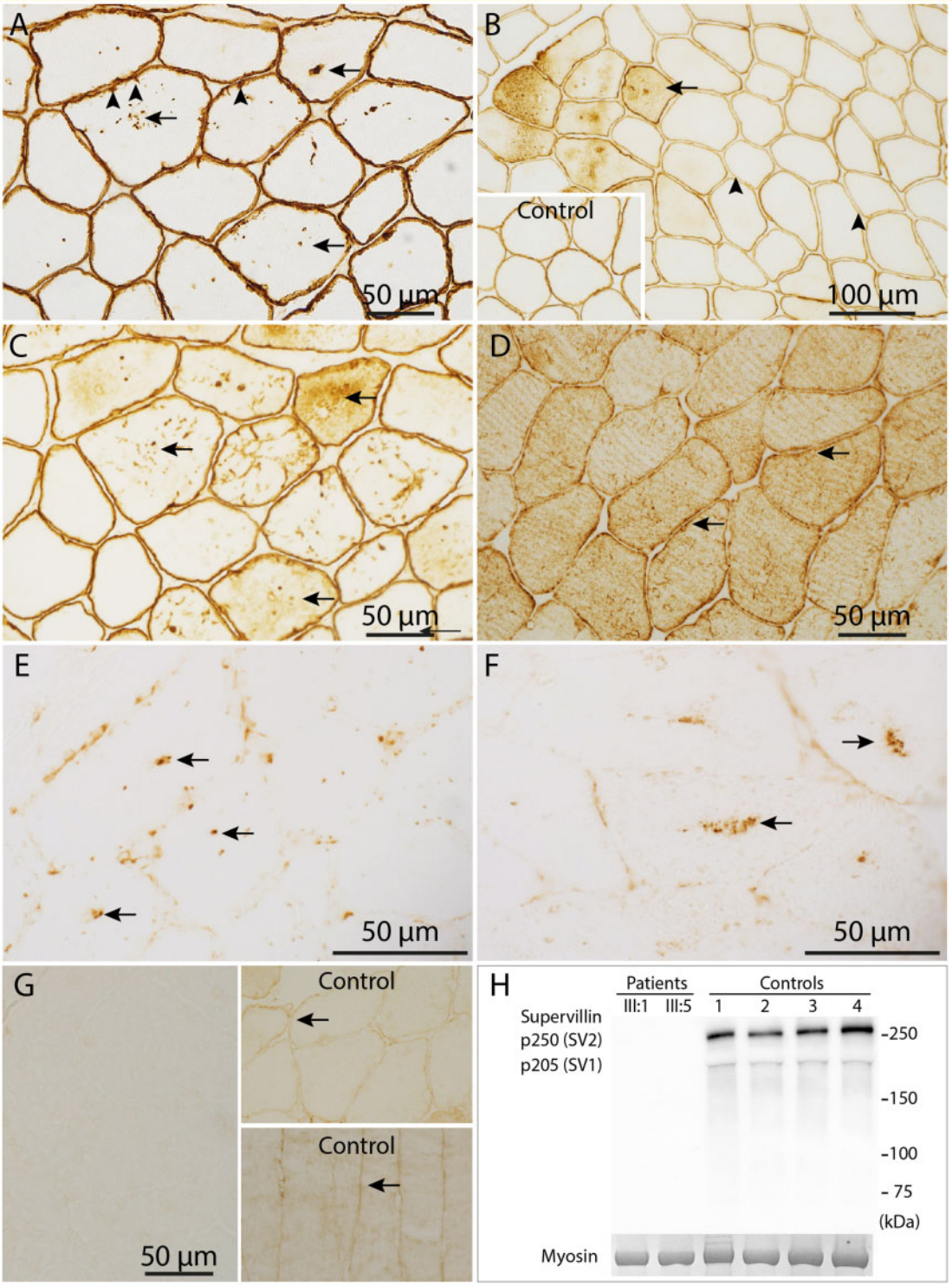

Figure 4 Immunohistochemical staining of muscle biopsy from Patient III:1 and western blot analysis of Patients III:1 and III:5 in Family 1. (**A**) α-Sarcoglycan appears focally accumulated in the subsarcolemmal region (arrow heads) and also internally (arrows) in several fibres. (**B**) Caveolin-3 shows variable and reduced staining at the sarcolemma (arrow heads) compared to a control (inset) and is also located in the interior of some fibres (arrows). (**C**) Dystrophin is distributed diffusely in the interior of several fibres (arrows) in the same region as illustrated in **A**. (**D**) Desmin is accumulated in the subsarcolemmal region in many fibres (arrows). (**E**) LAMP2 is present in association with several vacuoles indicating lysosomal origin (arrows). (**F**) LC3 is upregulated and present in the interior of some fibres (arrows). (**G**) Supervillin is completely absent compared to controls where it can be detected mainly in the sarcolemmal region (arrows). (**H**) Western blot analysis showing that supervillin is present in two isoforms, 250 kDa and 205 kDa, respectively, in controls but is completely absent in Patients III:1 and III:5. No truncated proteins were detected in the patients.

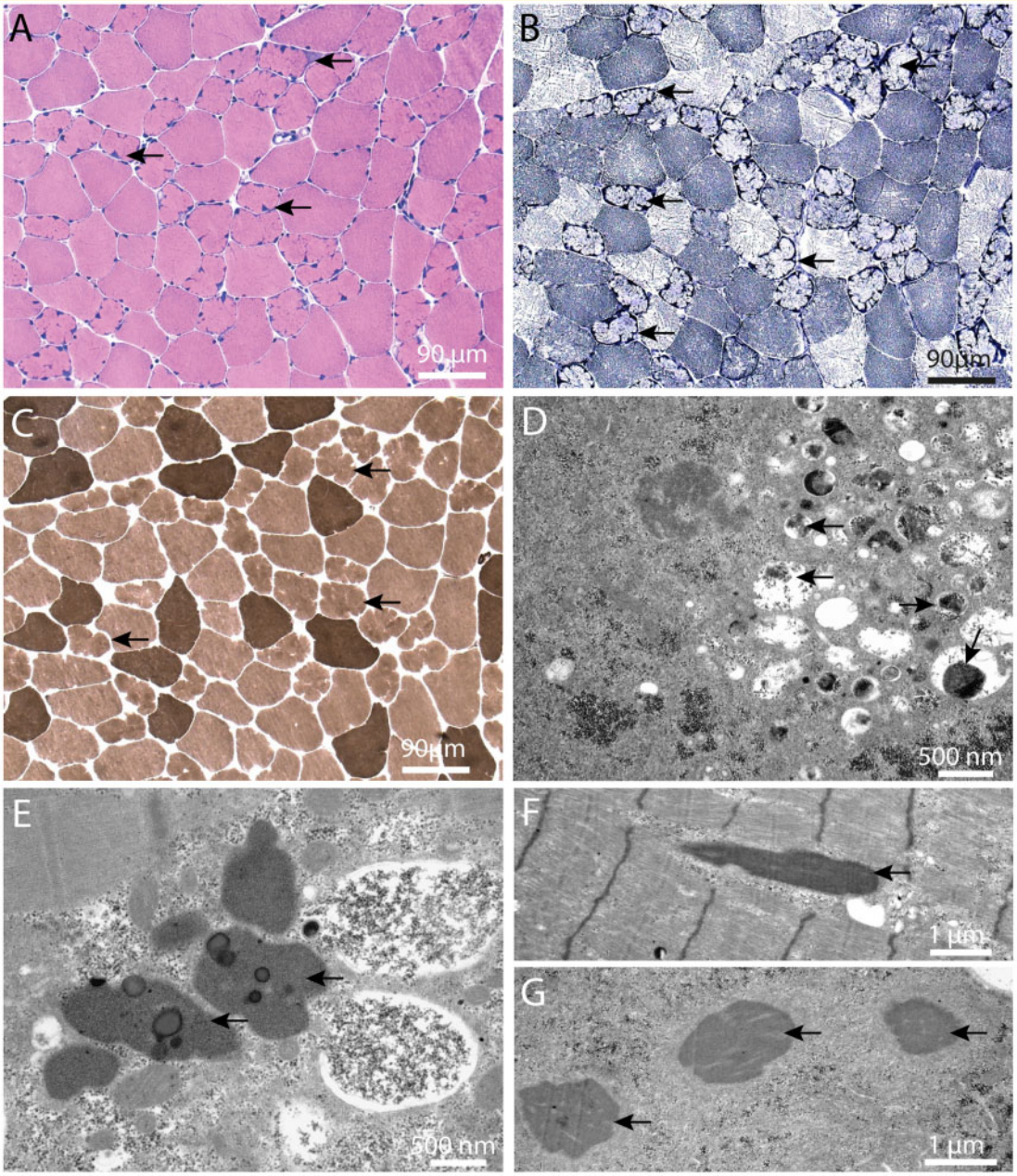

Figure 5 Biopsy from the deltoid muscle of Patient III:2 in Family 2, as visualized by light (A–C) and electron microscopy (D–G). (**A**) A considerable number of partially atrophic lobulated muscle fibres with pointed, occasionally cap-like subsarcolemmal deposits (arrows) (H&E). (**B**) Prominent oxidative enzyme activity in these fibres (arrows) (NADH). (**C**) Atrophic lobulated fibres are almost exclusively type I fibres (arrows); no neurogenic pattern is observed (mATPase at pH 9.4). (**D**) Subsarcolemmal accumulation of degraded myofibrils, glycogen, pleomorphic material and autophagy-associated (arrows) organelles. (**E**) Heterogeneous lipoprotein deposits including maturing lipofuscin (arrows). (**F**) Sporadically, nemaline rods are seen (arrow). (**G**) Three rods in transverse section (arrows).

In Family 2, a homozygous frameshift mutation in exon 18, c.3578_3579del, p.Val1193Glufs*46 in *SVIL* was identified (Fig. 7B and D). The mutation is absent from current human variation databases and is predicted to lead to a premature stop codon. No other obvious pathogenic variants were detected in genes previously linked to muscular diseases.

Protein expression of supervillin was studied by western blot analysis of skeletal muscle tissue in all four patients (Figs 4H, 6H and Supplementary Fig. 3), using antibodies with epitopes proximal to the truncating mutations. These analyses revealed a total absence of the full-length protein in affected patients whereas control samples showed two bands at 205 kDa and 250 kDa, respectively.

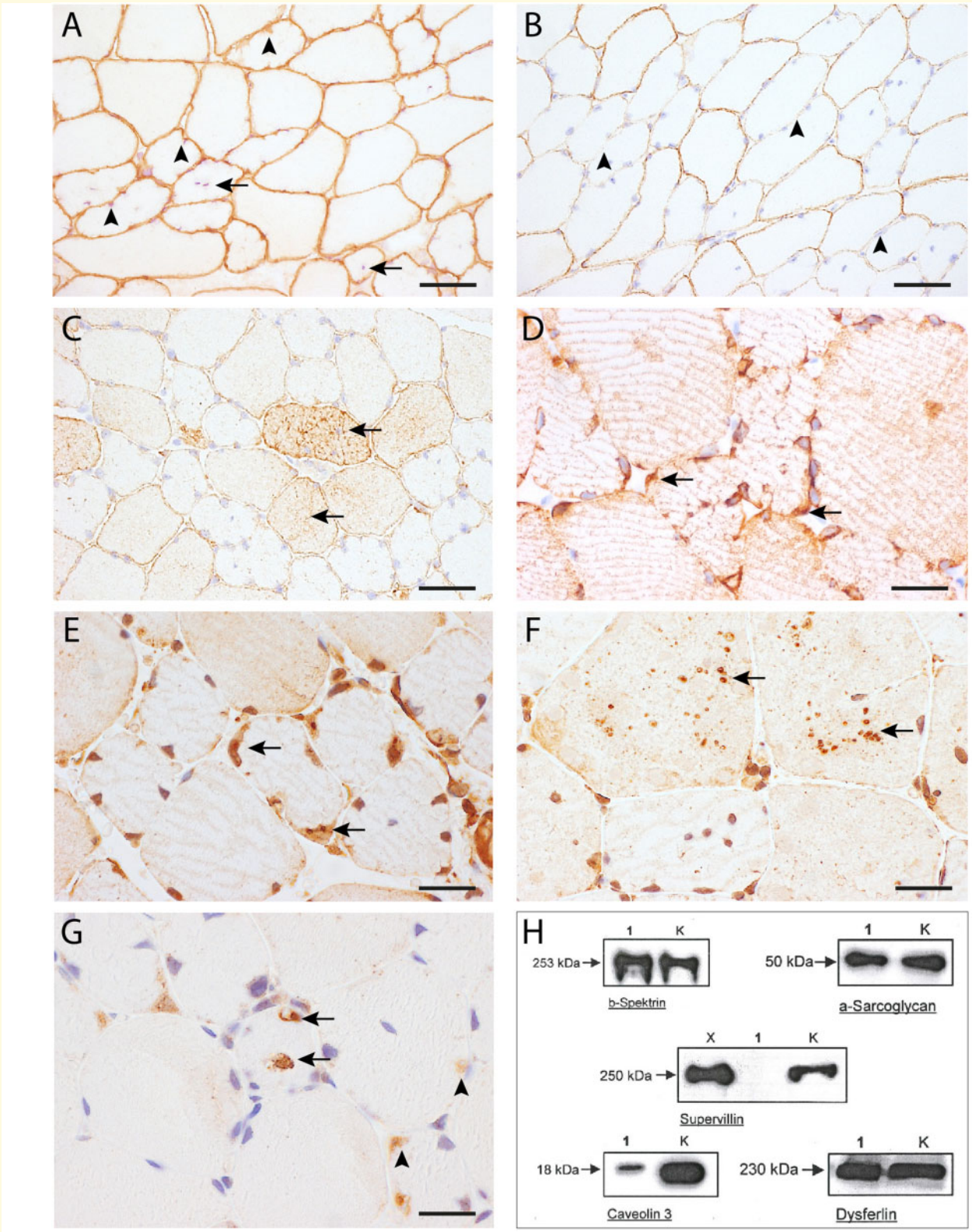

Figure 6 Immunohistochemical staining and western blot analysis of muscle biopsy from Patient III:3 in Family 2. (**A**) α-Sarcoglycan immunoreactivity of the pointy sarcolemma-associated structures in the lobulated muscle fibres (arrowheads) and internally in some fibres (arrows). (**B**) Irregular, reduced caveolin-3 staining mostly of smaller, partially atrophic fibres (arrowheads). (**C**) Abnormal non-sarcolemmal dysferlin immunoreactivity in several fibres (arrows). Subsarcolemmal accumulation of desmin (arrows) (**D**) and LC3 (arrows) (**E**) immunoreactivity in affected partially atrophic fibres. (**F**) LC3-positive granular and vacuolar structures (arrows) were also present in muscle fibres of normal size and in hypertrophic fibres. (**G**) Subsarcolemmal p62-immunoreactive subsarcolemmal material in affected lobulated fibres and occasional strongly stained p62-positive autophagic vacuoles (arrows). (**H**) Selected immunoblot results. I = index case; X and K = control cases. Scale bar = 40 μm in **A**–**C**, 25 μm in **D**–**G.**

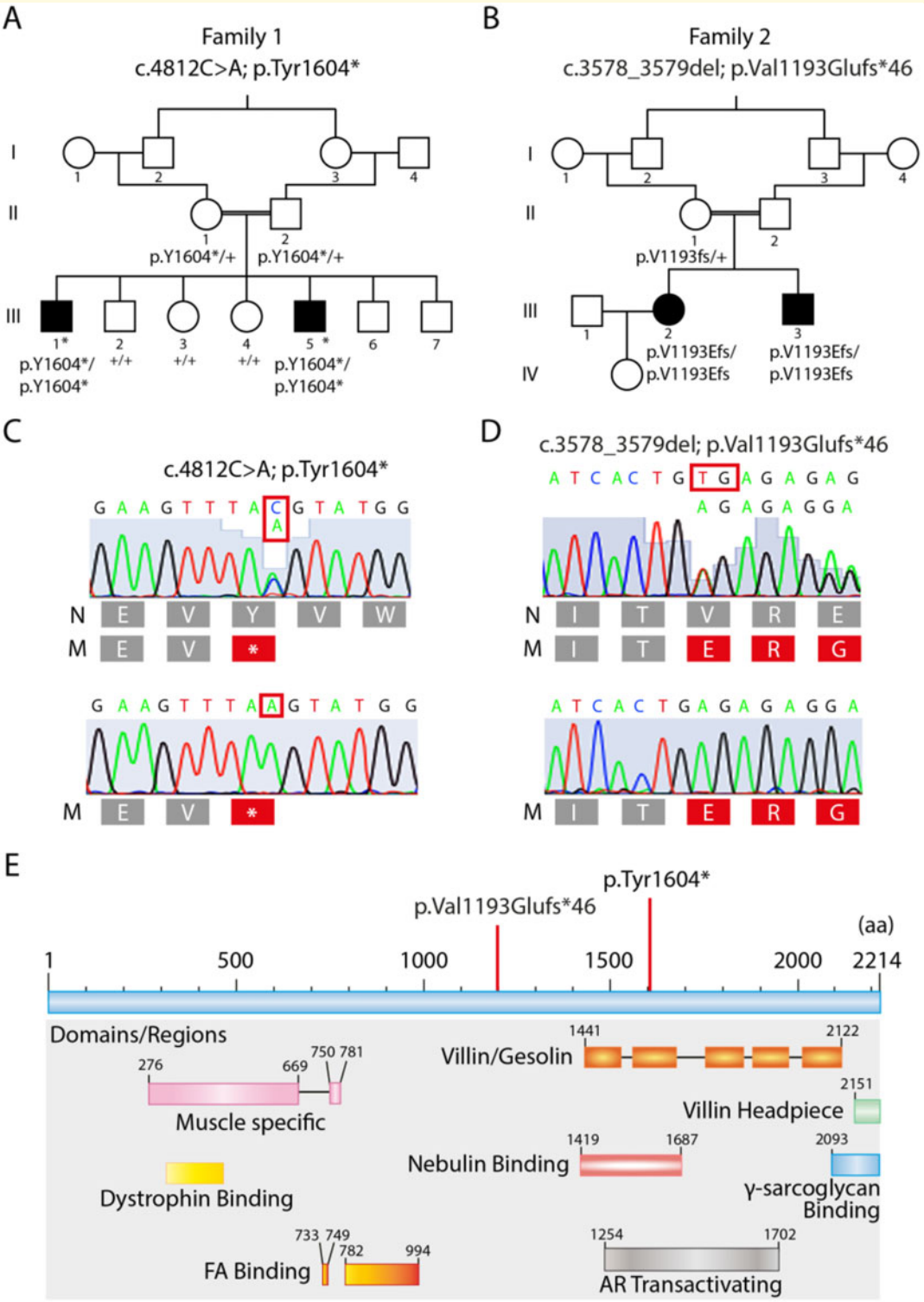

Figure 7 Pedigrees and molecular genetics. (**A**) Pedigree of Family 1. (**B**) Pedigree of Family 2. (**C**) Sequencing chromatograms demonstrating the homozygous mutation identified in Family 1 on genomic DNA, c.4812C > A; p.Tyr1604*. (**D**) Sequencing chromatograms demonstrating the homozygous mutation identified in Family 2 on genomic DNA, c.3578_3579del; p.Val1193Glufs*46. (**E**) Overview of the protein structure of supervillin isoform 2 (SV2, p250) and localization of the *SVIL* mutations described in this study. AR = androgen receptor; FA = focal adhesion; M = mutated sequence; N = normal sequence.

Discussion

We describe four patients from two families with a distinct myopathy and provide evidence that homozygous loss-of-function mutations in the *SVIL* gene cause a human cardiac and skeletal muscular disorder. In Family 1, a nonsense mutation (c.4812C>A; p.Tyr1604*) and in Family 2 a 2-bp deletion resulting in a frameshift and premature stop codon (c.3578_3579del; p.Val1193Glufs*46) were identified. Both reported mutations were shown to exert a loss-of-function effect. The mutations segregated with the disorder in both families, and none of the mutations has so far been identified in genome aggregation databases such as gnomAD. No homozygous loss-of-function mutations in *SVIL* have been reported in a large cohort of more than 60 000 unrelated individuals listed in the gnomAD database, suggesting that carriers of homozygous loss-of-function mutations of *SVIL* show phenotypic abnormalities and were therefore not included in the underlying large sequencing studies. This is also supported by a low ratio [0.26 (0.19–0.36, 90% confidence interval)] of the observed/expected number of loss-of-function mutations in that gene according to genome aggregation data (Karczewski *et al.*, 2019). The c.4812C>A; p.Tyr1604* mutation undergoes nonsense-mediated mRNA decay shown by PCR experiments, and loss of full-length supervillin proteins was shown in muscle tissue from both affected families. In the Genotype-Tissue Expression (GTEx) Portal Database (http://www.gtexportal.org) *SVIL* shows the highest expression in skeletal muscle, followed by other organs containing smooth muscle cells and cardiac muscle (Supplementary Fig. 2A), supporting a role for this protein in muscle. In non-muscle tissues, supervillin mRNAs are most abundantly expressed in thyroid gland, salivary gland and bone marrow, while expression in brain and liver is low (Pope *et al.*, 1998).

A wide neck and variable hypertrophy of trapezius and other back muscles were characteristic features of the patients in both families, together with moderately elevated creatine kinase levels. However, phenotypic differences were observed between the two families. Evidence of cardiac involvement but only mild contractures were present in Family 1. Family 2 showed progressive contractures and muscle stiffness, but only subclinical cardiac involvement in the form of slight left ventricular hypertrophy and elevated NT-proBNP. These differences in the intra- and interfamilial clinical presentation and age at onset are well known for other muscular disorders, for example in Bethlem myopathy (contractures; Bonnemann, 2011) or limb-girdle muscular dystrophies (cardiac involvement; Hermans *et al.*, 2010). Our patients did not show other obvious clinical manifestations in organs containing smooth muscle cells (e.g. gastrointestinal symptoms). These results are consistent with functional overlap between supervillin and other proteins, as documented in non-muscle cells (Crowley *et al.*, 2009; Smith *et al.*, 2013).

Muscle biopsies from both families revealed striking similarities and showed signs of a structural myopathy with numerous lobulated type 1 muscle fibres and myofibrillar alterations. Autophagic vacuoles, as well as frequent and extensive deposits of lipoproteins were observed as signs of altered proteostasis and impaired autophagy. The distinct histological and ultrastructural findings in both families suggest that this subtype of myopathy may be recognizable from muscle biopsies.

Supervillin is a large multi-domain protein (Fig. 7E). At least five different isoforms arising from differential splicing of 35 coding exons have been described (Chen *et al.*, 2003, 2017; Oh *et al.*, 2003; Gangopadhyay *et al.*, 2004; Fang and Luna, 2013). In non-muscle cells, the most abundant isoform is a 205-kDa protein that is encoded by 31 exons (SV1) (Pestonjamasp *et al.*, 1997). In cardiac and skeletal muscle, the most prominently expressed isoform is supervillin (SV2), which is the longest known muscle-specific isoform with a molecular mass of 250 kDa (Pope *et al.*, 1998; Oh *et al.*, 2003) (Supplementary Fig. 2B). The *SVIL* SV2 cDNA contains an initial muscle-specific 5′ leader sequence and four additional coding exons, which result in the N-terminal insert of the muscle specific amino acids 276–669 and 750–781 (Oh *et al.*, 2003). The locations of the mutations in our families, as well as our western blot data, suggest that all isoforms of supervillin are disrupted. Supervillin co-localizes with F-actin, vinculin and non-muscle myosin II at the membrane in myoblasts, and the protein is localized at the ends of differentiating myotubes (Oh *et al.*, 2003). The N-terminus common to supervillin SV1 and SV2 binds directly to smooth and non-muscle myosin II heavy chains and increases myosin II contractility (Chen *et al.*, 2003; Takizawa *et al.*, 2007; Bhuwania *et al.*, 2012; Edelstein *et al.*, 2012). A sequence in supervillin that is interrupted by the second muscle-specific insert regulates focal adhesion dynamics in non-muscle cells; its functionality in muscle is unknown (Takizawa *et al.*, 2006). Non-muscle and muscle isoforms share a central, conserved sequence that transactivates the androgen receptor (Ting *et al.*, 2002). Highly conserved *SVIL*-encoded C-terminal sequences interact with the C-terminus of nebulin and thus could attach supervillin (SV2) directly to the Z-line (Lee *et al.*, 2008). A previous study (Spinazzola *et al.*, 2015) has shown a physical interaction either via direct interaction or indirect association between the intracellular portion of γ-sarcoglycan and the C-terminus of supervillin (SV2) (Fig. 7E). Furthermore, the muscle-specific insert of supervillin binds to dystrophin (Fig. 7E) (Spinazzola *et al.*, 2015), and supervillin (SV2) and dystrophin co-localize at costameres in skeletal muscle (Oh *et al.*, 2003). The supervillin (SV2) muscle-specific domain also contains sequences homologous to those in supervillin SV3 (expressed in smooth muscle) that activate ERK signalling (Gangopadhyay *et al.*, 2009). Thus, supervillin (SV2) may coordinate both Z-line attachment to sarcomeres and signalling cross-talk between the dystrophin-glycoprotein complex and integrin-associated sarcomeric domains and between these domains and the nucleus. Such multiple functions of supervillin isoforms with both signalling and

structural properties may explain the characteristic muscle phenotypes in our patients.

In a proteomic study applying laser microdissection and mass spectrometry analyses on a protein aggregate myopathy caused by mutations in myotilin, supervillin was identified among the accumulated proteins (Maerkens *et al.*, 2016). Most of the accumulated proteins in the aggregates were Z-disc associated proteins followed by sarcolemmal and extracellular matrix proteins. It is therefore not surprising that supervillin was identified in the aggregates, probably because it binds to several of the accumulated proteins such as dystrophin and sarcoglycans. These results emphasize the role of supervillin as a binding partner to other structural proteins and thus probably functioning as part of a system keeping the essential components of muscle cells in their correct position. Complete loss of supervillin as indicated from the muscle biopsies from the affected patients was accompanied by alterations of major sarcolemma-associated proteins like caveolin-3, dystrophin, dysferlin and α-sarcoglycan as shown by immunohistochemistry. This may lead to changes of the muscle fibre cytoskeleton causing myofibrillar disarray and thus increased breakdown of myofibrillar proteins, resulting in altered proteostasis and impaired autophagy.

The heart involvement in Family 1 was mild and was mainly manifested by troponin T leakage and ECG abnormalities. By applying the Objective Prioritization Enhanced Novelty (OPEN) machine learning approach, *SVIL* was identified as a prioritized gene for dilated cardiomyopathy (Deo *et al.*, 2014). Using this approach *SVIL* was identified among three prioritized genes that were not previously associated with cardiac disease. A morpholino knock-down of *SVIL* in a zebrafish model demonstrated a significant decrease in atrial conduction velocity (Deo *et al.*, 2014). Results from these studies focusing on the heart support the concept that supervillin is of importance for normal cardiac function, but the exact physiological role of supervillin in the heart remains to be established.

In conclusion, this study reveals that biallelic loss-of-function mutations in *SVIL* cause a new structural myopathy with prominent lobulated type 1 fibres, myofibrillar disintegration and signs of altered proteostasis and impaired autophagy. Essential clinical signs of this new disorder include muscle pain and slowly progressive stiffness, contractures of varying degree, distinct anomalies of neck and shoulder girdle and mild cardiac involvement. The pathological changes emphasize the role of supervillin in maintaining the structural integrity of the muscle fibres. Although there were some striking phenotypic similarities between affected individuals from two nonrelated families, identification of additional patients will reveal the full phenotypic spectrum of this entity.

Acknowledgements

We thank Brith Leidvik and Hannelore Mader for excellent technical assistance, Bong-Sung Kim for performing muscle biopsy of Family 2 and Thomas Eggermann and Herdit Schüler for cytogenetic and molecular genetic workup of the patients.

Funding

This study was supported by the Swedish Research Council to A.O. (grant number 2018-02821) and by the German Research Foundation (DFG) to I.K. (KU1587/4-1).

Competing interests

The authors report no competing interests.

Supplementary material

Supplementary material is available at *Brain* online.

References

Bhuwania R, Cornfine S, Fang Z, Kruger M, Luna EJ, Linder S. Supervillin couples myosin-dependent contractility to podosomes and enables their turnover. J Cell Sci 2012; 125: 2300–14.

Bonnemann CG. The collagen VI-related myopathies Ullrich congenital muscular dystrophy and Bethlem myopathy. Handb Clin Neurol 2011; 101: 81–96.

Chen Y, Takizawa N, Crowley JL, Oh SW, Gatto CL, Kambara T, et al. F-actin and myosin II binding domains in supervillin. J Biol Chem 2003; 278: 46094–106.

Chen X, Yang H, Zhang S, Wang Z, Ye F, Liang C, et al. A novel splice variant of supervillin, SV5, promotes carcinoma cell proliferation and cell migration. Biochem Biophys Res Commun 2017; 482: 43–9.

Crowley JL, Smith TC, Fang Z, Takizawa N, Luna EJ. Supervillin reorganizes the actin cytoskeleton and increases invadopodial efficiency. MBoC 2009; 20: 948–62.

Deo RC, Musso G, Tasan M, Tang P, Poon A, Yuan C, et al. Prioritizing causal disease genes using unbiased genomic features. Genome Biol 2014; 15: 534.

Dubowitz V, Sewry CA, Oldfors A, Muscle biopsy: a practical approach. 4th edn. Philadelphia: Elsevier; 2013.

Edelstein LC, Luna EJ, Gibson IB, Bray M, Jin Y, Kondkar A, et al. Human genome-wide association and mouse knockout approaches identify platelet supervillin as an inhibitor of thrombus formation under shear stress. Circulation 2012; 125: 2762–71.

Fang Z, Luna EJ. Supervillin-mediated suppression of p53 protein enhances cell survival. J Biol Chem 2013; 288: 7918–29.

Fang ZY, Takizawa N, Wilson KA, Smith TC, Delprato A, Davidson MW, et al. The membrane-associated protein, supervillin, accelerates F-actin-dependent rapid integrin recycling and cell motility. Traffic 2010; 11: 782–99.

Gangopadhyay SS, Kengni E, Appel S, Gallant C, Kim HR, Leavis P, et al. Smooth muscle archvillin is an ERK scaffolding protein. J Biol Chem 2009; 284: 17607–15.

Gangopadhyay SS, Takizawa N, Gallant C, Barber AL, Je HD, Smith TC, et al. Smooth muscle archvillin: a novel regulator of signaling and contractility in vascular smooth muscle. J Cell Sci 2004; 117: 5043–57.

Guo Y, Ding X, Shen Y, Lyon GJ, Wang K. SeqMule: automated pipeline for analysis of human exome/genome sequencing data. Sci Rep 2015; 5: 14283.

Hermans MC, Pinto YM, Merkies IS, de Die-Smulders CE, Crijns HJ, Faber CG. Hereditary muscular dystrophies and the heart. Neuromuscul Disord 2010; 20: 479–92.

Jaka O, Casas-Fraile L, De Munain AL, Saenz A. Costamere proteins and their involvement in myopathic processes. Expert Rev Mol Med 2015; 17:

Karczewski KJ, Francioli LC, Tiao G, Cummings BB, Alföldi J, Wang Q, et al. Variation across 141,456 human exomes and genomes reveals the spectrum of loss-of-function intolerance across human protein-coding genes bioRxiv 2019.

Lee MA, Joo YM, Lee YM, Kim HS, Kim JH, Choi JK, et al. Archvillin anchors in the Z-line of skeletal muscle via the nebulin C-terminus. Biochem Biophys Res Commun 2008; 374: 320–4.

Lee YM, Kim HS, Choi JH, Choi JK, Joo YM, Ahn SJ, et al. Knockdown of archvillin by siRNA inhibits myofibril assembly in cultured skeletal myoblast. J Exp Biomed Sci 2007; 251–61.

Li MX, Gui HS, Kwan JS, Bao SY, Sham PC. A comprehensive framework for prioritizing variants in exome sequencing studies of Mendelian diseases. Nucleic Acids Res 2012; 40: e53.

Maerkens A, Olive M, Schreiner A, Feldkirchner S, Schessl J, Uszkoreit J, et al. New insights into the protein aggregation pathology in myotilinopathy by combined proteomic and immunolocalization analyses. Acta Neuropathol Commun 2016; 4: 8.

Nigro V, Piluso G. Spectrum of muscular dystrophies associated with sarcolemmal-protein genetic defects. Biochim Biophys Acta 2015; 1852: 585–93.

Oh SW, Pope RK, Smith KP, Crowley JL, Nebl T, Lawrence JB, et al. Archvillin, a muscle-specific isoform of supervillin, is an early expressed component of the costameric membrane skeleton. J Cell Sci 2003; 116: 2261–75.

Pestonjamasp KN, Pope RK, Wulfkuhle JD, Luna EJ. Supervillin (p205): a novel membrane-associated, F-actin-binding protein in the villin/gelsolin superfamily. J Cell Biol 1997; 139: 1255–69.

Pope RK, Pestonjamasp KN, Smith KP, Wulfkuhle JD, Strassel CP, Lawrence JB, et al. Cloning, characterization, and chromosomal localization of human superillin (SVIL). Genomics 1998; 52: 342–51.

Romero NB, Clarke NF. Congenital myopathies. Handb Clin Neurol 2013; 113: 1321–36.

Smith TC, Fang ZY, Luna EJ. Novel Interactors and a Role for Supervillin in Early Cytokinesis. Cytoskeleton 2010; 67: 346–64.

Smith TC, Fridy PC, Li Y, Basil S, Arjun S, Friesen RM, et al. Supervillin binding to myosin II and synergism with anillin are required for cytokinesis. MBoC 2013; 24: 3603–19.

Spinazzola JM, Smith TC, Liu M, Luna EJ, Barton ER. Gamma-sarcoglycan is required for the response of archvillin to mechanical stimulation in skeletal muscle. Hum Mol Genet 2015; 24: 2470–81.

Takizawa N, Ikebe R, Ikebe M, Luna EJ. Supervillin slows cell spreading by facilitating myosin II activation at the cell periphery. J Cell Sci 2007; 120: 3792–803.

Takizawa N, Smith TC, Nebl T, Crowley JL, Palmieri SJ, Lifshitz LM, et al. Supervillin modulation of focal adhesions involving TRIP6/ZRP-1. J Cell Biol 2006; 174: 447–58.

Ting HJ, Yeh S, Nishimura K, Chang C. Supervillin associates with androgen receptor and modulates its transcriptional activity. Proc Natl Acad Sci U S A 2002; 99: 661–6.